


ORIGINAL ARTICLE

Heat shock protein 90 inhibitors induce cell differentiation via the ubiquitin-dependent aurora kinase A degradation in a MPLW515L mouse model of primary myelofibrosis

Fuping Wang¹ | Haotian Zhang¹ | Binghong He¹ | Zihan Liu¹ | Xinxin Wu¹ |
Yuankai Liu¹ | Xin Xu¹ | Xiaoxue Gou¹ | Haitao Wang² | Qiong Yang¹ 

¹Beijing Key Laboratory of Gene Resource and Molecular Development, College of Life Sciences, Beijing Normal University, Beijing, China

²Department of Hematology, Fifth Medical Center, Chinese PLA General Hospital, Beijing, China

Correspondence

Qiong Yang, Beijing Key Laboratory of Gene Resource and Molecular Development, College of Life Sciences, Beijing Normal University, Beijing 100000, China.
Email: yangqiong@bnu.edu.cn

Funding information

Natural Science Foundation of China Beijing Municipality, Grant/Award Number: 2202021; National Natural Science Foundation of China, Grant/Award Numbers: 21773015, 22072005

Abstract

Primary myelofibrosis (PMF) is characterized by immature megakaryocytic hyperplasia, splenomegaly, extramedullary hematopoiesis and bone marrow fibrosis. Our preclinical study had demonstrated that aurora kinase A (AURKA) inhibitor MLN8237 reduced the mutation burden of PMF by inducing differentiation of immature megakaryocytes. However, it only slightly alleviated splenomegaly, reduced tissue fibrosis, and normalized megakaryocytes in PMF patients of the preliminary clinical study. So enhancing therapeutic efficacy of PMF is needed. In this study, we found that AURKA directly interacted with heat shock protein 90 (HSP90) and HSP90 inhibitors promoted the ubiquitin-dependent AURKA degradation. We demonstrated that HSP90 inhibitors 17-allylamino-17-demethoxygeldanamycin (17-AAG) and 17-dimethylaminoethylamino-17-demethoxygeldanamycin (17-DMAG), normalized peripheral blood counts, improved splenomegaly, attenuated extramedullary hematopoiesis, decreased tissue fibrosis and reduced mutant burden in a MPLW515L mouse model of PMF. Importantly, both 17-AAG and 17-DMAG treatment at effective doses *in vivo* did not influence on hematopoiesis in healthy mice. Collectively, the study demonstrates that HSP90 inhibitors induce cell differentiation via the ubiquitin-dependent AURKA and also are safe and effective for the treatment of a MPLW515L mouse model of PMF, which may provide a new strategy for PMF therapy. Further, we demonstrate that combined therapy shows superior activity in acute megakaryocytic leukemia mouse model than single therapy.

KEYWORDS

aurora kinase A, differentiation, heat shock protein 90, megakaryocyte, primary myelofibrosis

1 | INTRODUCTION

Primary myelofibrosis (PMF) affects about one in 100,000 people worldwide.^{1–3} Worse, 10%–20% of PMF patients may transform to acute megakaryocytic leukemia (AMKL) and then have a medium overall survival of 5.8 months.⁴ Immature megakaryocytic

hyperplasia was the typical feature of PMF patients and these immature megakaryocytes played an important role in the disease progression and pathologic formation of PMF.⁵ Our previous study had proved that high level and activation of aurora kinase A (AURKA) was crucial for the expansion of immature megakaryocytes in PMF, and AURKA inhibitor MLN8237 reduced the

mutation burden by inducing differentiation of immature megakaryocytes.⁶ However, a primarily clinical trial reported that MLN8237 only slightly alleviated splenomegaly, reduced tissue fibrosis and normalized megakaryocytes in PMF patients.² Due to the limited efficacy of MLN8237 for PMF patients, it is necessary to further investigate the maintenance mechanism of high AURKA level and to find new differentiated therapeutic targets. The discovery of novel targets may provide new avenues of single-agent and combinatorial therapy for PMF patients.

In this study, we found that AURKA directly interacted with heat shock protein 90 (HSP90) and its inhibitors promoted the ubiquitin-dependent AURKA degradation. Then, we investigated the effects of HSP90 inhibitors on proliferation and differentiation of human erythroleukemia (HEL) cells and mouse primary bone marrow c-Kit⁺ cells bearing *MPLW515L* mutation. Further, HSP90 inhibitors, 17-allylamino-17-demethoxygeldanamycin (17-AAG) and 17-dimethylaminoethylamino-17-demethoxygeldanamycin (17-DMAG) were evaluated in the *MPLW515L* mouse model of PMF (*MPLW515L* mouse). Toxicity was tested at the dose effective treatment in mice. In addition, we demonstrated that combined 17-DMAG and MLN8237 showed superior activity in AMKL mouse model than single therapy. The study provided a promising treatment for PMF and AMKL with *MPLW515L* mutation.

2 | MATERIALS AND METHODS

2.1 | Cell culture

Mouse primary bone marrow c-Kit⁺ cells were cultured in StemSpan medium supplemented with 10 ng/ml mouse interleukin-3 (IL-3), 10 ng/ml human IL-6 and 40 ng/ml mouse stem cell factor, along with 20 µg/ml human low density lipoprotein.⁶ HEL cells were grown in RPMI 1640 medium supplemented with 10% FBS and 100 mg/ml penicillin-streptomycin mix.⁶ HEK293T cells were grown in DMEM medium supplemented with 10% FBS, 1% L-glutamine and 100 mg/ml penicillin-streptomycin mix.^{7,8}

2.2 | Liquid chromatography coupled with tandem mass spectrometry (LC-MS/MS)

AURKA-FLAG HEK293T cells (HEK293T were transduced with the lentivirus expressing AURKA-FLAG fusion protein) and FLAG HEK293T cells (HEK293T cells were transduced with the lentivirus expressing FLAG) were lysed in RIPA buffer supplemented with protease inhibitors. Lysates of AURKA-FLAG HEK293T cells and FLAG HEK293T cells were immunoprecipitated with ANTI-FLAG[®] M2 Affinity Gel (Sigma), respectively.⁹ Immunoprecipitates from AURKA-FLAG HEK293T cells and FLAG HEK293T cells were separated by SDS-PAGE. SDS-PAGE gel was dyed with 0.25% coomassie brilliant blue. These SDS-PAGE gel bands of two immunoprecipitates were analysis by LC-MS/MS.¹⁰

2.3 | Western blots

HEL cells were harvested after treatment with the indicated concentrations of 17-AAG (Selleck) for 24 h. AURKA-FLAG HEL cells were incubated with DMSO or 10 µM 17-AAG/NVP-AUY922 and/or 10 µM MG-132 for 24 h. Cell lysates were separated on SDS-PAGE gels, transferred to PVDF membranes, and blotted with human AURKA antibody (GeneTex) and human HSC70 antibody (Santa Cruz).⁶

2.4 | Co-immunoprecipitation

AURKA-FLAG HEL cells or FLAG HEL cells (HEL cells were transduced with the lentivirus expressing FLAG) were lysed in RIPA buffer supplemented with protease inhibitors.⁶ These lysates of AURKA-FLAG HEL cells or FLAG HEL cells were immunoprecipitated with ANTI-FLAG[®] M2 Affinity Gel or IgG-Agarose (Sigma). The immunoprecipitates were separated on SDS-PAGE gel, transferred to PVDF membrane, and blotted with human HSP90α/β antibody (Santa Cruz) and ANTI-FLAG[®] M2 antibody (M2) (Sigma).⁹ Besides, lysates of AURKA-FLAG HEL cells or FLAG HEL cells were used as input controls.

2.5 | Ubiquitin-immunoprecipitation

AURKA-FLAG HEL cells were incubated with DMSO or 10 µM 17-AAG and/or 10 µM MG-132 for 24 h. AURKA-FLAG HEL cells were lysed in RIPA buffer supplemented with protease inhibitors.⁶ These lysates were immunoprecipitated with ANTI-FLAG[®] M2 Affinity Gel or IgG-Agarose. The immunoprecipitates were separated on SDS-PAGE gel, transferred to PVDF membrane, and blotted with human Ubiquitin antibody (Santa Cruz). Besides, cell lysates were blotted with ANTI-FLAG[®] M2 antibody and human HSC70 antibody.⁹

2.6 | Trypan blue staining for analyzing cell growth

HEL cells were incubated with DMSO or the indicated concentrations of 17-AAG for 24, 48 and 72 h. After incubation, cell viability was assessed using trypan blue staining. The primary cells were transduced with retroviral expressing *MPLW515L* protein. They were incubated with DMSO or the indicated concentrations of 17-AAG in the presence of 10 ng/ml mouse THPO for 24, 48 and 72 h.⁶ Further, half maximal inhibitory concentration (IC₅₀) of the cells was determined.

2.7 | Quantitative RT-PCR

HEL cells were incubated with DMSO or the indicated concentrations of 17-AAG for 48 h. HEL cells were harvested and RNA was extracted using TransGen EasyPure Blood RNA Kit. RNA was reverse transcribed to cDNA using PrimeScript[™] RT Reagent Kit.¹¹

Quantitative RT-PCR assays were performed using TB Green Premix Ex Taq II.

2.8 | Flow cytometry

HEL cells were incubated with DMSO or the indicated concentrations of 17-AAG for 72 h and then stained using human antibodies CD41a (BD Biosciences) and CD42a (BD Biosciences) for 30 min in PBS staining buffer. Mouse primary bone marrow c-Kit⁺ cells were transduced with retrovirus expressing MPLW515L and GFP proteins. Then, the cells were cultured in the presence of DMSO or the indicated concentrations of 17-AAG for 72 h. Finally, the cells stained using mouse antibody CD41 (Invitrogen) for 30 min in PBS staining buffer.⁶ For the analysis of megakaryocytic population, bone marrow and spleen cells from MPLW515L mice or healthy mice were stained using mouse antibody CD41 and Hoechst 33,342 (Invitrogen). For the analysis of granulocytes, bone marrow and spleen cells from MPLW515L mice or healthy mice were stained using mouse antibodies Gr-1 (Invitrogen) and CD11b (BD Biosciences). For the analysis of erythroid precursors, bone marrow and spleen cells from MPLW515L mice or healthy mice were stained using mouse antibodies Ter119 (BD Biosciences) and CD71 (BD Biosciences). For the analysis of myeloid progenitor populations, bone marrow and spleen cells from MPLW515L mice or healthy mice were stained using mouse biotin-labeled anti-mouse antibodies including mouse Ly-6G/Ly-6C monoclonal antibody (Invitrogen), TER-119 monoclonal antibody (Invitrogen), CD11b monoclonal antibody (Invitrogen), CD3e monoclonal antibody (Invitrogen), and CD45R monoclonal antibody (Invitrogen). These cells were stained with Streptavidin PerCP-Cyanine55 conjugate (Invitrogen). Then, these samples were stained with anti-mouse monoclonal antibodies including c-Kit-APC-eFluor 780 (Invitrogen), Sca-1-PE (Invitrogen), CD34-Alexa Fluor[®] 647 (BD Biosciences), and CD16/CD32-PE-Cyanine7 (Invitrogen) to analyze myeloid progenitor populations, including common myeloid progenitors (CMP), granulocyte-macrophage progenitors (GMP), and megakaryocyte-erythroid progenitors (MEP).¹²

2.9 | Bone marrow transplantation

Seven-week-old recipient C57BL/6NCrI female mice that were lethally irradiated with 950 cGy and then transplanted with mouse primary bone marrow c-Kit⁺ cells transduced with retrovirus expressing MPLW515L via tail vein. For the therapeutic study of 17-AAG, recipient C57BL/6NCrI mice were transplanted with the transduced mouse primary bone marrow c-Kit⁺ cells that contained 3×10^5 GFP⁺ cells via tail vein. Seven days after transplantation, recipient mice were treated every 2 days for 16 days with vehicle or 25 mg/kg 17-AAG by intraperitoneal injection and were examined after 22 days of transplantation.^{13,14} For the therapeutic study of 17-DMAG, recipient C57BL/6NCrI mice were transplanted with the transduced mouse primary bone marrow c-Kit⁺ cells that contained

2.7×10^5 GFP⁺ cells via tail vein. Nine days after transplantation, recipient mice were treated every 2 days for 20 days with vehicle or 10 mg/kg 17-DMAG by intraperitoneal injection and were examined after 28 days of transplantation.^{15,16} Seven-week-old recipient C57BL/6NCrI female mice that were lethally irradiated with 450 cGy and then transplanted with 6133/MPL cells via tail vein. For the combination therapy of 17-DMAG and MLN8237, recipient C57BL/6NCrI mice were transplanted with 1×10^6 6133/MPL cells via tail vein. Seven days after transplantation, recipient mice were treated five times for 9 days with 5 mg/kg 17-DMAG by intraperitoneal injection and seven times for 9 days with vehicle (15 mg/ml arginine) or 5 mg/kg MLN8237 by oral gavage. These recipient mice were examined after 15 days of transplantation.^{6,17}

2.10 | HSP90 inhibitor treatment of healthy mice

Healthy C57BL/6NCrI mice were treated with vehicle (0.5% (w/v) Pluronic F68 and 0.5% (w/v) PVP-K30), 25 mg/kg 17-AAG or 10 mg/kg 17-DMAG by intraperitoneal injection every 3 days and examined for 22 days.⁶

2.11 | Complete blood counts

Blood (50 μ L) was collected from the tail vein in EDTA-coated tubes and analyzed by a MEK-6410C automatic blood cell analyzer.

2.12 | Histopathology

Blood smears were fixed in methanol and stained in Giemsa stain solution.¹⁸ Spleen, liver, and sternum were fixed in 4% fixative solution and then embedded in paraffin. Paraffin-embedded tissue sections were stained with Hematoxylin-Eosin and Gordon-Sweets.^{6,19} The degree of fibrosis was assessed by pathologists blinded to specific treatment groups using the Image Pro plus 6.0, according to the World Health Organization's score.

3 | RESULTS

3.1 | AURKA interacts with HSP90

First, LC-MS/MS assay identified 220 proteins that specifically interacted to AURKA (Figure 1A). Enrichment analysis of molecular function showed that 220 AURKA interacting proteins were enriched in chaperone activity, translation regulator activity and ubiquitin-specific protease activity (Figure 1B). Enrichment analysis of biological process showed that 220 AURKA interacting proteins were significantly related to protein metabolism (Figure 1C). Then, KEGG pathway analysis by DAVID showed that 220 AURKA interacting proteins were significantly related to proteasome pathway

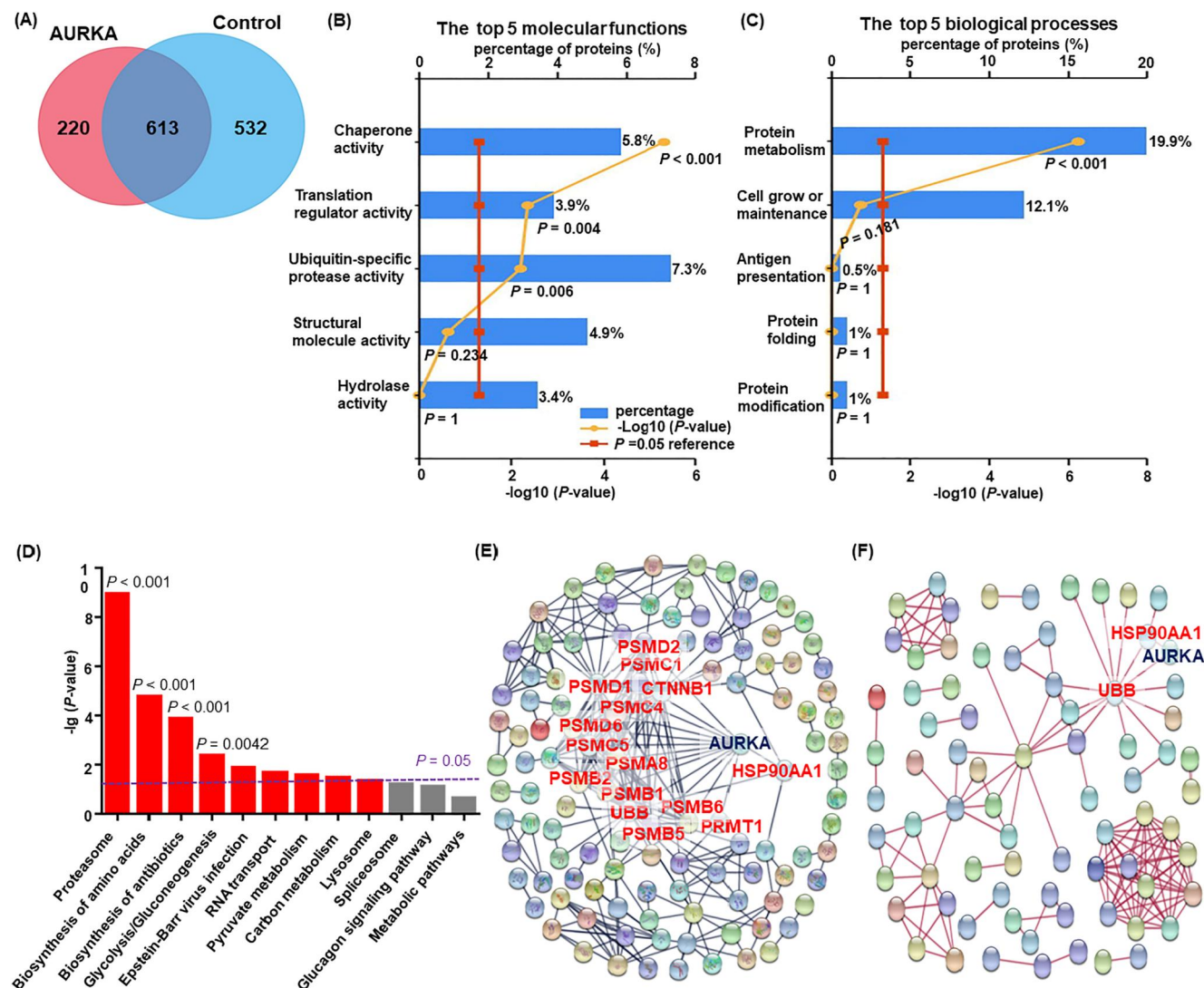


FIGURE 1 Proteomic analyses of aurora kinase A (AURKA) complexes by liquid chromatography coupled with tandem mass spectrometry (LC-MS/MS) reveals that AURKA associates with heat shock protein 90 (HSP90). (A) Venn diagram showed the unique 220 AURKA interacting proteins compared to the control. AURKA complexes were extracted from HEK293T cells that transduced with lentivirus expressing AURKA-FLAG fusion protein. Control complexes were extracted from HEK293T cells that transduced with lentivirus expressing FLAG. AURKA and control complexes were immunoprecipitated by using ANTI-FLAG® M2 Affinity Gel, respectively. Then the complexes were run in SDS-PAGE and then the gels were cut into small pieces for MS analysis. Protein sequences identified by LC-MS/MS were compared to uniprot_human database (<https://www.uniprot.org/>). (B) Molecular function enrichment analysis of 220 AURKA interacting proteins in AURKA complexes by FunRich software. 220 AURKA interacting proteins were significantly related to chaperone activity, translation regulator activity and ubiquitin-specific protease activity ($p < 0.001$). (C) Biological process enrichment analysis of 220 AURKA interacting proteins in AURKA complexes by FunRich software. 220 AURKA interacting proteins were significantly related to protein metabolism ($p < 0.001$). (D) KEGG pathway analysis of 220 AURKA interacting proteins in AURKA complexes by DAVID (<https://david.ncifcrf.gov/>). 220 AURKA interacting proteins were significantly related to proteasome pathway ($p < 0.001$). (E) Full network analysis of 220 AURKA interacting proteins revealed that AURKA associated with 15 proteins by STRING (<https://string-db.org/>). 11 of 15 proteins were proteasomal component proteins, and the other four proteins were HSP90AA1, PRMT1, CTNNB1 and UBB. (F) Physical network analysis of 220 AURKA interacting proteins revealed that AURKA formed a physical complex with HSP90AA1 and UBB by STRING. Interactions with required interaction score (≥ 0.900) were represented. Each node represented a protein and disconnected nodes were hidden.

(Figure 1D). Full network analysis of 220 AURKA interacting proteins revealed AURKA associated with 15 proteins (Figure 1E). Finally, physical network analysis of 220 AURKA interacting proteins revealed that AURKA formed a physical complex with HSP90AA1 and UBB (Figure 1F). These results showed that HSP90 were associated with AURKA.

3.2 | HSP90 inhibitors promote the ubiquitin-dependent AURKA degradation

In AURKA-FLAG HEL cells, the immunoprecipitate from IP of FLAG detected AURKA-FLAG and HSP90; whereas the immunoprecipitate from IP of IgG couldn't detect AURKA-FLAG and

HSP90. In FLAG HEL cells, immunoprecipitates from IP of FLAG and IP of IgG couldn't detect AURKA-FLAG and HSP90. Therefore, these results demonstrated that AURKA directly interacted with HSP90 (Figure 2A). Further, 17-AAG efficaciously depleted AURKA level in a dose-dependent manner in HEL cells (Figure 2B). When treated with MG-132, AURKA-FLAG HEL cell prominently increased AURKA level (Figure 2C,D). When treated with 17-AAG or NVP-AUY922, AURKA-FLAG HEL cell prominently increased AURKA expression in the presence of MG-132 compared to the controls (Figure 2C,D). Under the treatment of MG-132, we observed that 17-AAG obviously increased the AURKA ubiquitination level compared to the control without 17-AAG (Figure 2E). These findings demonstrated that HSP90 inhibitors resulted in degradation of AURKA by ubiquitin-proteasome pathway.

3.3 | HSP90 inhibitor inhibits proliferation and induces differentiation in HEL cells and mouse primary bone marrow c-Kit⁺ cells bearing MPLW515L mutation

17-AAG could significantly inhibit the proliferation of HEL cells in a dose-dependent manner (Figure 3A). CD41 and CD42 were considered as primary criteria for megakaryocyte differentiation. When treated with 17-AAG, both CD41 and CD42 expression of HEL cells in the mRNA level increased and showed a dose-dependent trend (Figure 3B,C). Furthermore, when treated with 17-AAG, both CD41 (Figure 3D,E) and CD42 (Figure 3F,G) expression of HEL cells in the protein level were also significantly increased. These findings validated that 17-AAG induced megakaryocyte differentiation in HEL cells.

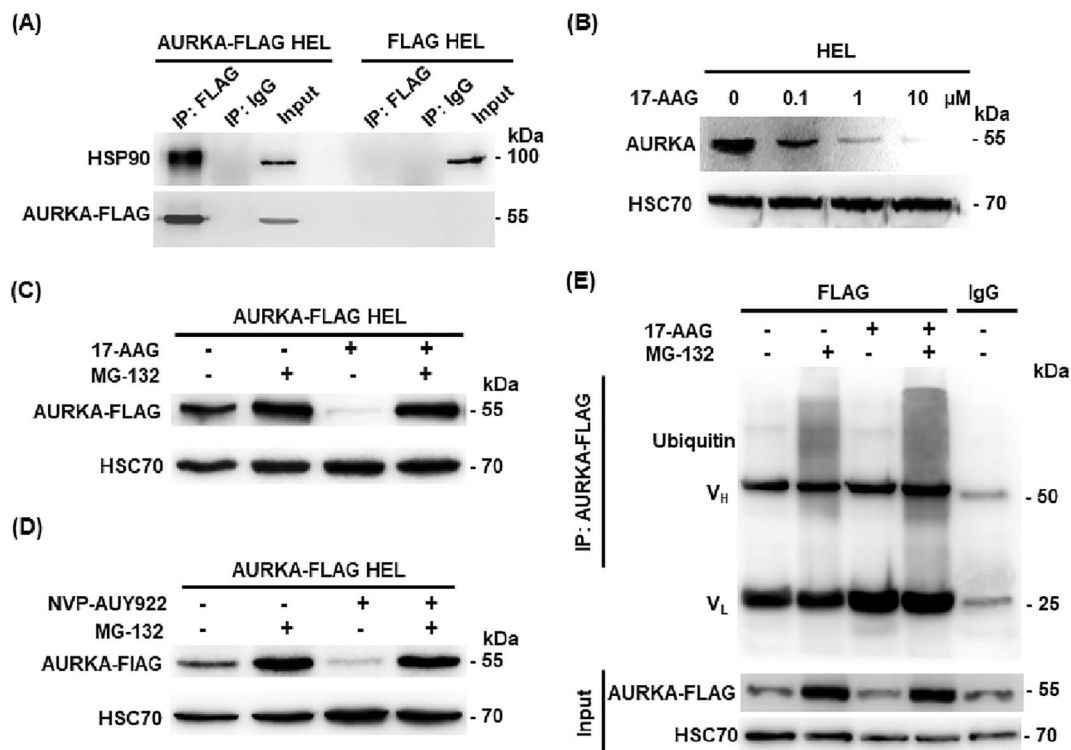


FIGURE 2 Aurora kinase A (AURKA) directly interacts with heat shock protein 90 (HSP90) and is degraded via the ubiquitin-proteasome pathway. Human erythroleukemia (HEL) cells were transduced with lentivirus expressing AURKA-FLAG fusion protein (AURKA-FLAG HEL cells). (A) Lysates of AURKA-FLAG HEL cells or FLAG HEL cells were immunoprecipitated with ANTI-FLAG[®] M2 Affinity Gel or IgG-Agarose. The immunoprecipitates were respectively immunoblotted with human HSP90 α/β (F-8) antibody and ANTI-FLAG[®] M2 antibody. Besides, lysates of AURKA-FLAG HEL cells or FLAG HEL cells were used as input controls. (B) Western blot analysis of HEL cells incubated with 17-AAG or DMSO for 24 h. HSC70 served as a loading control. (C) Western blot analysis of AURKA-FLAG HEL cells incubated 10 μ M 17-AAG and/or 10 μ M MG-132 for 24 h. HSC70 served as a loading control. (D) Western blot analysis of AURKA-FLAG HEL cells incubated 10 μ M NVP-AUY922 and/or 10 μ M MG-132 for 24 h. HSC70 served as a loading control. (E) HSP90 inhibitor promoted the ubiquitin-dependent AURKA degradation. AURKA-FLAG HEL cells incubated 10 μ M 17-AAG and/or 10 μ M MG-132 for 24 h. Lysates of AURKA-FLAG HEL cells were immunoprecipitated with ANTI-FLAG[®] M2 Affinity Gel or IgG-Agarose. The immunoprecipitates were immunoblotted with Ubiquitin (P4D1) antibody. Besides, lysates of AURKA-FLAG HEL cells were immunoblotted with ANTI-FLAG[®] M2 antibody and human HSC70 (B-6) antibody.

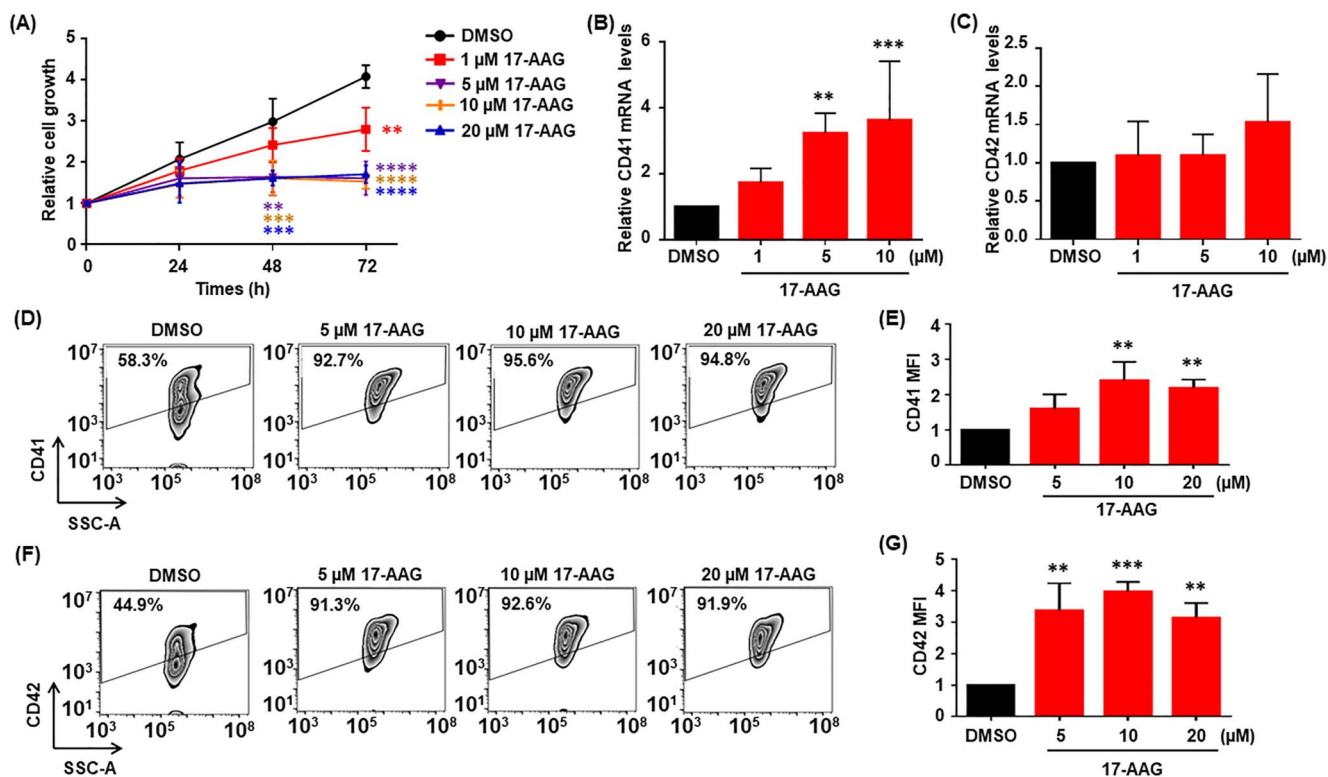


FIGURE 3 Heat shock protein 90 (HSP90) inhibitor inhibits proliferation and induces differentiation in human erythroleukemia (HEL) cells. (A) Cell counting of HEL cells that were cultured in the presence of DMSO or the indicated concentrations of 17-AAG for 24, 48 and 72 h, respectively. (B) The mRNA level of CD41 in HEL cells that were cultured in the presence of DMSO or the indicated concentrations of 17-AAG for 48 h. (C) The mRNA level of CD42 in HEL cells that were cultured in the presence of DMSO or the indicated concentrations of 17-AAG for 48 h. (D) Flow cytometry plots of cells showing CD41 expression for HEL cells that were cultured in the presence of DMSO or the indicated concentrations of 17-AAG for 72 h. (E) CD41 mean fluorescence intensity (MFI) of HEL cells that were cultured in the presence of DMSO or the indicated concentrations of 17-AAG for 72 h. (F) Flow cytometry plots of cells showing CD42 expression in HEL cells that were cultured in the presence of DMSO or the indicated concentrations of 17-AAG for 72 h. (G) CD42 MFI of HEL cells that were cultured in the presence of DMSO or the indicated concentrations of 17-AAG for 72 h. Error bars represent mean \pm SD. p values by two-way ANOVA in A. p values by one-way ANOVA in B, C, E and G. ** $p < 0.01$, *** $p < 0.001$ and **** $p < 0.0001$, as compared to DMSO.

Meanwhile, we assessed the influence of HSP90 inhibitor 17-AAG on proliferation and differentiation of mouse primary bone marrow c-Kit⁺ cells bearing *MPLW515L* mutation. 17-AAG could significantly inhibit the proliferation of the primary cells in a dose-dependent manner (Figure S1A). The IC₅₀ value of 17-AAG for mouse primary bone marrow c-Kit⁺ cells bearing *MPLW515L* mutation was 393.2 nM (Figure S1B). Under the similar GFP expression of mouse primary bone marrow c-Kit⁺ cells bearing *MPLW515L* mutation, 17-AAG significantly induced CD41 expression of the cells in a dose-dependent manner (Figure S1C,D). Therefore, 17-AAG inhibited proliferation and induced differentiation in mouse primary bone marrow c-Kit⁺ cells bearing *MPLW515L* mutation.

3.4 | 17-AAG or 17-DMAG doesn't affect hematopoietic composition and tissue structure in healthy mice

Healthy mice were treated every 3 days for 22 days with vehicle, 25 mg/kg 17-AAG or 10 mg/kg 17-DMAG by intraperitoneal injection and were examined for 22 days. 17-AAG or 17-DMAG

treatment of C57BL/6Ncr1 mice had no significant effect on body weight and peripheral blood (PB) cells (Figure 4A–E). Obviously, there weren't significant difference in spleen and liver sizes of wild-type (WT), vehicle, 17-AAG and 17-DMAG mice (Figure 4F,G). Moreover, histological analysis of the spleen, liver and bone marrow revealed that 17-AAG or 17-DMAG treatment at this dose didn't cause myelosuppression or other detrimental effects (Figure 4H–J). There weren't significant difference of CD41⁺ megakaryocytic cells, Gr1⁺ CD11b⁺ granulocyte cells and CD71⁺Ter119⁺ erythroid cells in bone marrow and spleen of WT, vehicle, 17-AAG and 17-DMAG mice (Figure S2A–L). Furthermore, there weren't significantly difference of CMP, GMP and MEP in bone marrow and spleen of WT, vehicle, 17-AAG and 17-DMAG mice (Figure S3A–D). Summarily, 17-AAG or 17-DMAG didn't affect hematopoietic composition in healthy mice.

3.5 | 17-AAG reduces disease burden in the *MPLW515L* mouse model of primary myelofibrosis

We measured GFP expression over time as a surrogate marker of disease burden for *MPLW515L* mutant cells (*MPLW515L* is expressed

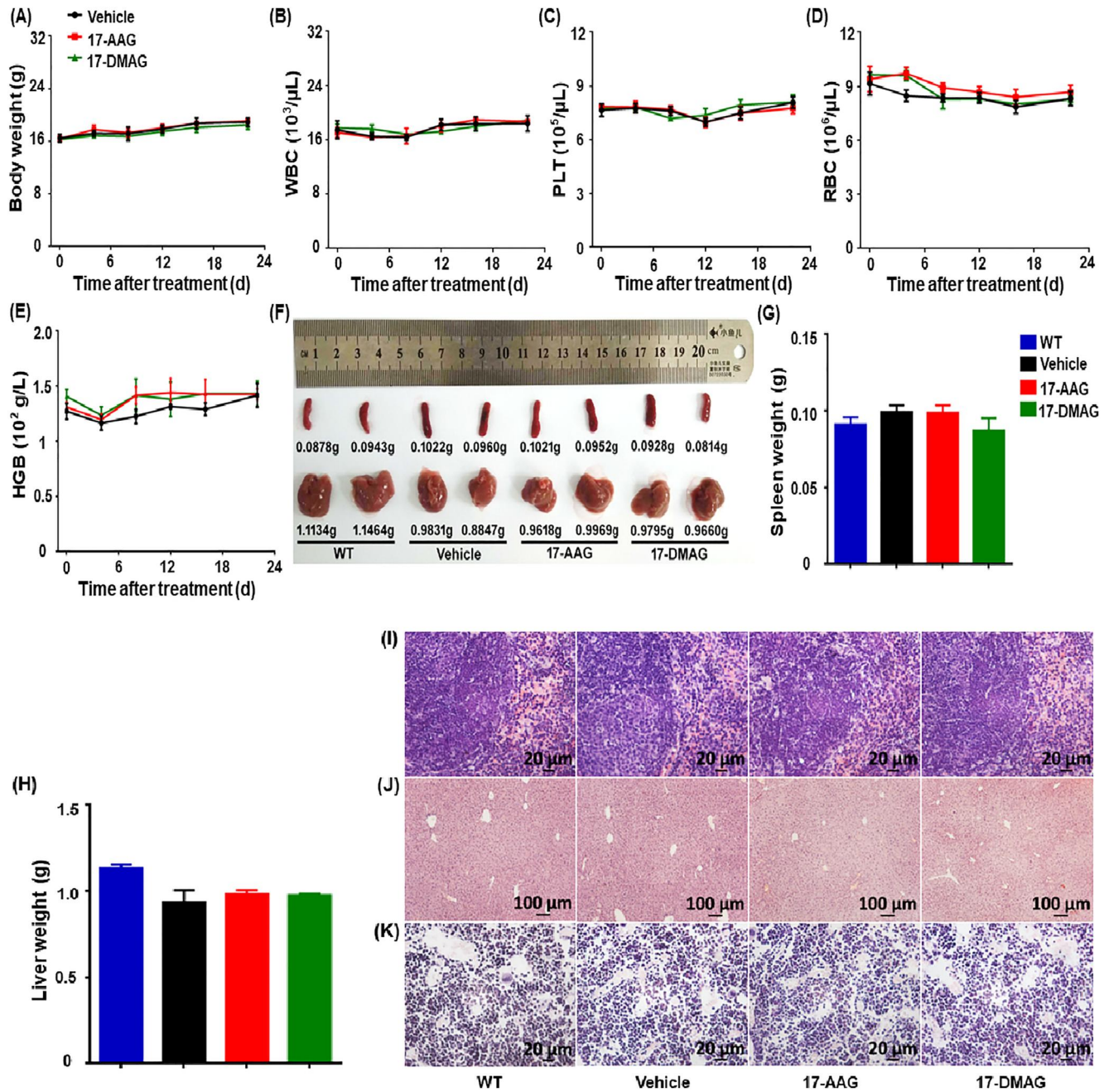


FIGURE 4 17-AAG or 17-DMAG doesn't affect hematopoietic composition and tissue structure in healthy mice. Healthy mice were treated every 3 days for 22 days with vehicle, 25 mg/kg 17-AAG or 10 mg/kg 17-DMAG by intraperitoneal injection and were examined for 22 days. (A) Body weight following treatment with 17-AAG or 17-DMAG versus vehicle. (B) White blood cell (WBC) counts in peripheral blood (PB). (C) Platelet counts in PB. (D) Red blood cell (RBC) counts in PB. (E) Hemoglobin (HGB) changes in PB. (F) The size of spleen and liver on day 22. (G) Spleen weight of every mouse on day 22. (H) Liver weight of every mouse on day 22. (I) H&E-stained sections of spleen. (J) H&E-stained sections of liver. (K) H&E-stained sections of sternum. $n = 4$ per group. Error bars in the graphs represent the mean \pm SD. p values by two-way ANOVA in A, B, C, D and E. p values by one-way ANOVA in G and H.

using a MSCV-IRES-GFP virus). Twenty-two days after transplantation of mouse primary bone marrow c-Kit⁺ cells bearing MPLW515L mutation to irradiated C57BL/6NcrJ recipient mice, we verified that all vehicle mice had >56% GFP⁺ cells in the PB and 17-AAG significantly reduced the GFP⁺ tumor cell population in the PB (Figure 5A). 17-AAG significantly reduced white blood cells

(Figures 5B,K and S4A) and platelets in the PB of MPLW515L mice (Figure 5C). In addition, 17-AAG decreased red blood cells and hemoglobin in PB of MPLW515L mice (Figure 5D,E). 17-AAG didn't change the body weight in MPLW515L mice (Figure 5F) and significantly reduced spleen and liver weights (Figure 5G-I). Further, 17-AAG treatment significantly decreased spleen total cells (Figure 5J).

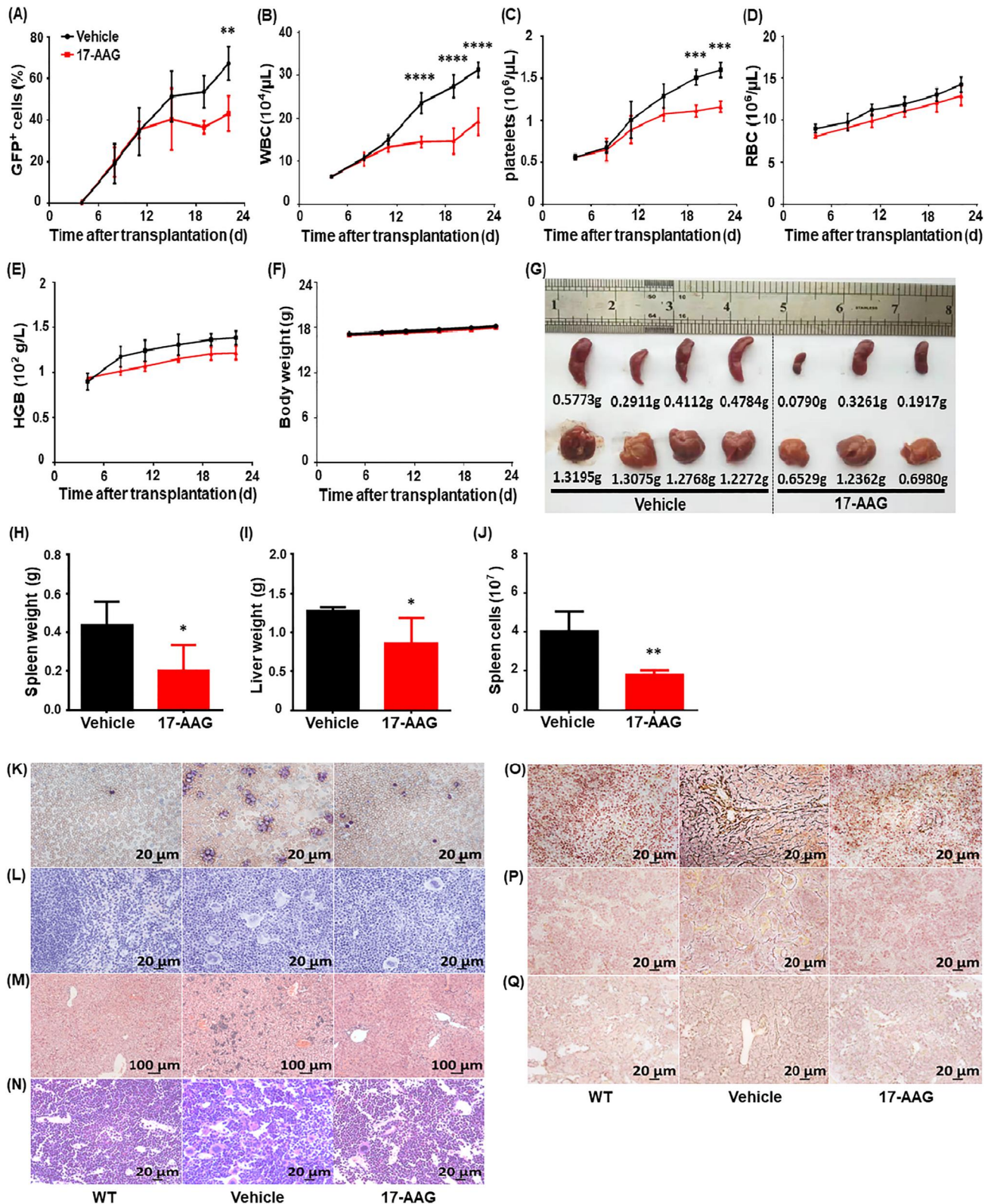


FIGURE 5 17-AAG reduces disease burden in peripheral blood (PB), spleen, liver and bone marrow of MPLW515L mouse model of primary myelofibrosis (PMF). MPLW515L bone marrow-recipient mice were treated every 2 days for 16 days with vehicle or 25 mg/kg 17-AAG by intraperitoneal injection and were examined after 22 days of transplantation. (A) Percentage of GFP⁺ cells in PB. (B) White blood cell (WBC) counts in PB. (C) Platelet counts in PB. (D) Red blood cell (RBC) counts in PB. (E) Hemoglobin (HGB) changes in PB. (F) Body weight following treatment with vehicle versus 17-AAG. (G) The sizes of spleens and livers on day 22. (H) Spleen weights of every mouse on day 22. (I) Liver weights of every mouse on day 22. (J) Spleen total cells in every mouse on day 22. (K) Giemsa-stained blood smears. (L) H&E-stained sections of spleen. (M) H&E-stained sections of liver. (N) H&E-stained sections of sternum. (O) Reticulin-stained sections of spleen. (P) Reticulin-stained sections of liver. (Q) Reticulin-stained sections of sternum. $n = 4$ per group. Error bars represent mean \pm SD. p values by two-way ANOVA in A, B, C, D, E and F. p values by unpaired two-sided Student's t -test in H, I and J. * $p < 0.05$, ** $p < 0.01$, *** $p < 0.001$ and **** $p < 0.0001$, as compared to vehicle.

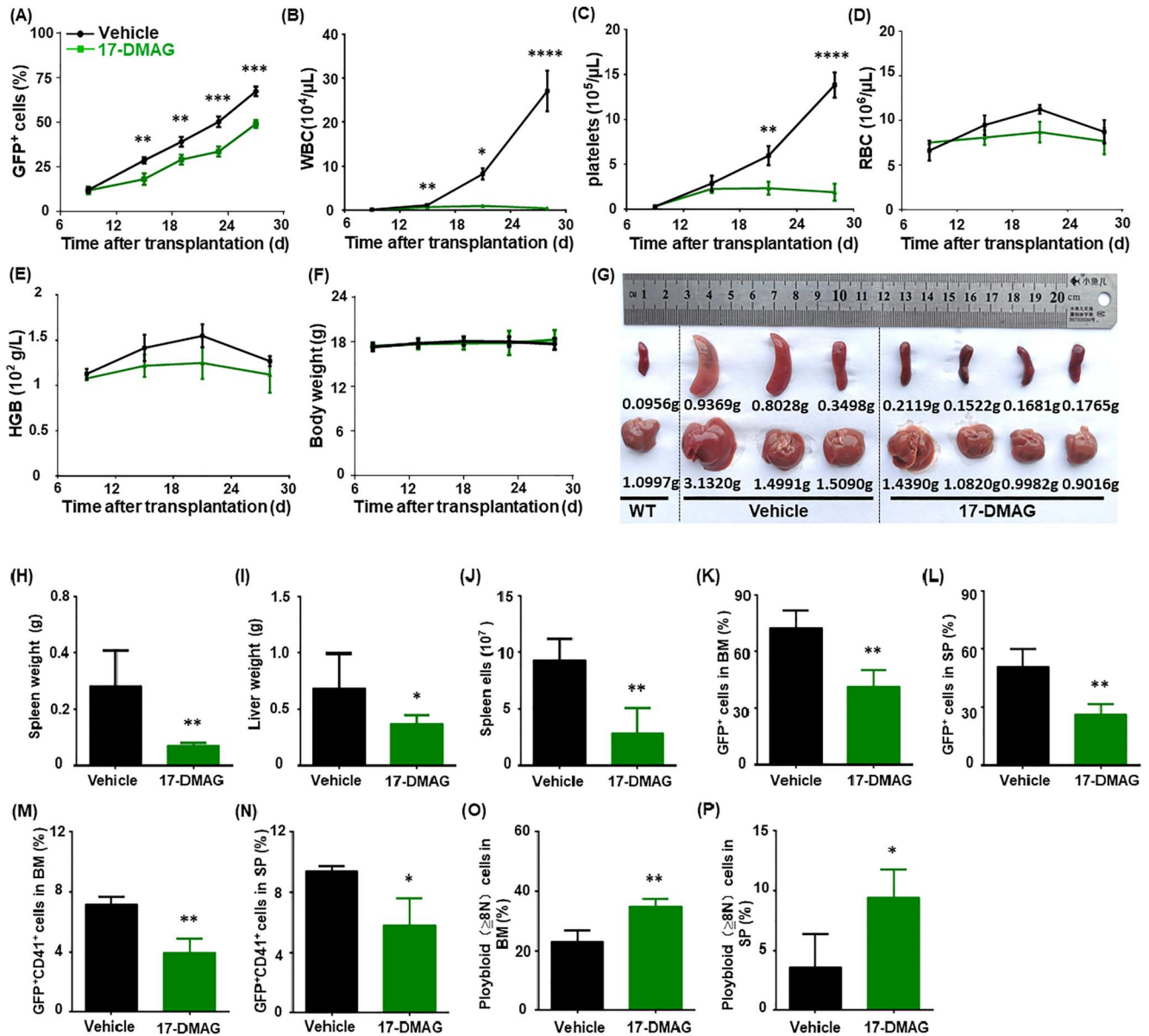


FIGURE 6 17-DMAG reduces disease burden in peripheral blood (PB), spleen, liver and bone marrow in the MPLW515L mouse model of primary myelofibrosis (PMF). MPLW515L bone marrow-recipient mice were treated every 2 days for 20 days with vehicle or 10 mg/kg 17-DMAG by intraperitoneal injection and were examined after 28 days of transplantation. (A) Percentage of GFP⁺ cells in PB. (B) White blood cell (WBC) counts in PB. (C) Platelet counts in PB. (D) Red blood cell (RBC) counts in PB. (E) Hemoglobin (HGB) changes in PB. (F) Body weight following treatment with vehicle versus 17-DMAG. (G) The size of spleen and liver in every mouse in day 28. (H) Spleen weight in every mouse in day 28. (I) Liver weight in every mouse in day 28. (J) Spleen total cells in every mouse in day 28. (K) Percentage of GFP⁺ cells in bone marrow of MPLW515L mice. (L) Percentage of GFP⁺ cells in spleen of MPLW515L mice. (M) Percentage of GFP⁺CD41⁺ cells in bone marrow of MPLW515L mice. (N) Percentage of GFP⁺CD41⁺ cells in spleen of MPLW515L mice. (O) Polyplody of GFP⁺ cells in bone marrow of MPLW515L mice. (P) Polyplody of GFP⁺ cells in spleen of MPLW515L mice. $n = 4$ per group. WT, wildtype. Error bars represent mean \pm SD. p values by two-way ANOVA in A, B, C, D, E and F. p values by unpaired two-sided Student's t -test in H, I, J, K, L, M, N, O and P. * $p < 0.05$, ** $p < 0.01$, *** $p < 0.001$ and **** $p < 0.0001$, as compared to vehicle.

Importantly, 17-AAG significantly reduced megakaryocytes in spleen and sternum of MPLW515L mice (Figures 5L,N and S4B,C). 17-AAG significantly relieved liver hematopoiesis in MPLW515L mice (Figure 5M). 17-AAG strikingly decreased spleen, liver and sternum fibrosis in MPLW515L mice (Figures 5O-Q and S4D-F). Therefore, our data demonstrated that 17-AAG reduced disease burden in PB, spleen and liver of MPLW515L mouse.

3.6 | 17-DMAG reduces disease burden in the MPLW515L mouse model of primary myelofibrosis

Twenty-eight days after transplantation of mouse primary bone marrow $c\text{-Kit}^+$ cells bearing MPLW515L mutation to irradiated C57BL/6NcrJ recipient mice, we verified that all vehicle mice had >60% GFP⁺ cells in the PB and 17-DMAG significantly reduced the

GFP⁺ tumor cell population in the PB (Figure 6A). 17-DMAG dramatically decreased white blood cells (Figures 6B, 7A and S11A) and platelets in the PB of MPLW515L mice (Figure 6C). In addition, 17-DMAG decreased red blood cells and hemoglobin in the PB of MPLW515L mice (Figure 6D,E). 17-DMAG didn't change the body weight in MPLW515L mice (Figure 6F) and significantly reduced spleen and liver weights (Figure 7G-I). 17-DMAG treatment reduced spleen total cells (Figure 6J). 17-DMAG could significantly alleviate the percentage of GFP⁺ cells in bone marrow and spleen of MPLW515L mice (Figures 6K-L, S5 and S6). Percentage of GFP⁺CD41⁺ cells and polyploid of GFP⁺ cells significantly reduced in bone marrow and spleen of MPLW515L mice after 17-DMAG treatment (Figures 6M-O and S7-S10). 17-DMAG significantly decreased megakaryocytes in the spleen and sternum of MPLW515L mice (Figures 7B,D and S11B,C) and liver hematopoiesis in MPLW515L mice (Figure 7C). Moreover, 17-DMAG strikingly decreased spleen, liver and sternum fibrosis in MPLW515L mice (Figures 7E-G and S11D-F). Altogether, 17-DMAG significantly reduced disease burden in PB, spleen, liver and bone marrow in MPLW515L mouse.

3.7 | 17-DMAG and MLN8237 enhanced the significance of reducing disease burden in the AMKL mouse model

Fifteen days after transplantation of 6133/MPL cells to irradiated C57BL/6NcrI recipient mice, we verified that all vehicle mice had >40% GFP⁺ cells in the PB and 17-DMAG or MLN8237 significantly

reduced the GFP⁺ tumor cell population in the PB (Figure 8A). 17-DMAG dramatically decreased white blood cells in the PB of AMKL mice (Figure 8B,G). Importantly, 17-DMAG didn't change the body weight in AMKL mice and significantly reduced spleen and liver weights (Figure 8C-F). Percentage of GFP⁺CD41⁺ cells and polyploid of GFP⁺ cells increased in bone marrow and spleen of AMKL mice after 17-DMAG and MLN8237 treatment (Figure S12A-D). Together, combined 17-DMAG and MLN8237 showed superior activity in the AMKL mouse than single therapy.

4 | DISCUSSION

HSP90 inhibitors have made progress in the study of many diseases, but its mechanism of HSP90 inhibitor needs further study.²⁰⁻²⁵ In this study, we showed that AURKA directly interacted with HSP90 and was protected from proteasomal degradation by HSP90. It suggested that HSP90 inhibition was a new strategy for patients with AURKA-dependent malignancies. At the 17-AAG and 17-DMAG concentrations we studied, 17-AAG or 17-DMAG doesn't affect hematopoietic composition and tissue structure in healthy mice. Our results demonstrated that 17-AAG and 17-DMAG significantly induced cell differentiation via the ubiquitin-dependent AURKA degradation in MPLW515L mouse. Importantly, 17-AAG and 17-DMAG reduced the mutation burden and tissue fibrosis in MPLW515L mouse. Furthermore, combination of 17-DMAG and MLN8237 showed superior activity in AMKL mice, it suggested that combined HSP90 inhibitor and AURKA inhibitor might have a better therapeutic effect on PMF and AMKL patients.

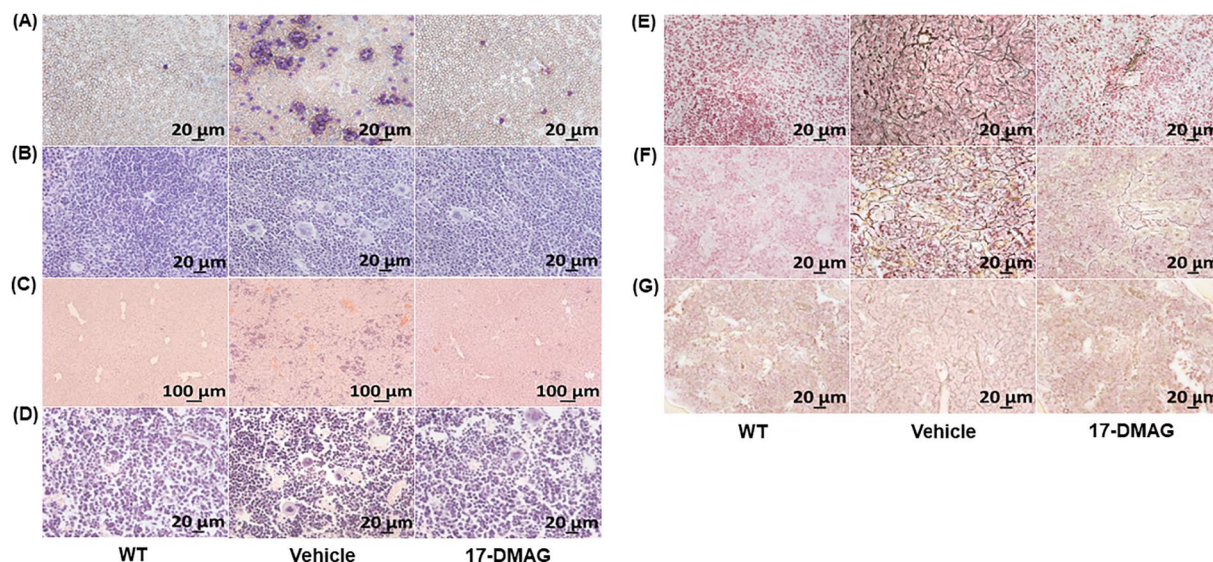


FIGURE 7 17-DMAG reduces disease burden in the MPLW515L mouse model of primary myelofibrosis (PMF) on histopathology. MPLW515L bone marrow-recipient mice were treated every 2 days for 20 days with vehicle or 10 mg/kg 17-DMAG by intraperitoneal injection and were examined for 28 days. (A) Giemsa-stained blood smears. (B) H&E-stained sections of spleen. (C) H&E-stained sections of liver. (D) H&E-stained sections of sternum. (E) Reticulin-stained sections of spleen. (F) Reticulin-stained sections of liver. (G) Reticulin-stained sections of sternum.

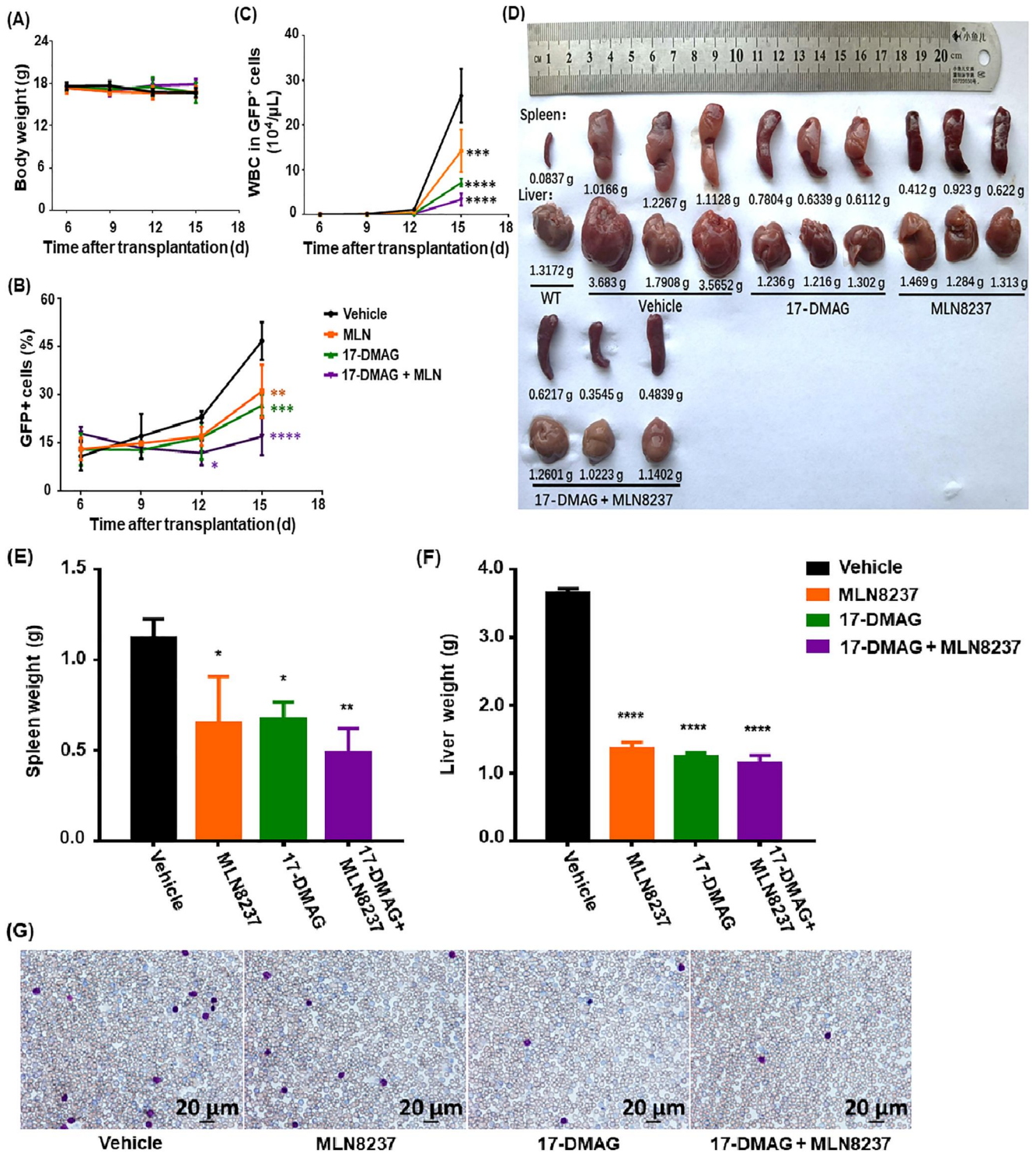


FIGURE 8 17-DMAG and MLN8237 enhanced the significance of reducing disease burden in the acute megakaryocytic leukemia (AMKL) mouse model. 6133/MPL cells-recipient mice were treated with vehicle, 5 mg/kg MLN8237, 5 mg/kg 17-DMAG or 5 mg/kg 17-DMAG and, 5 mg/kg MLN8237. 6133/MPL cells-recipient mice were examined for 15 days. (A) Body weight of AMKL mice. (B) Percentage of GFP⁺ cells in peripheral blood (PB) of AMKL mice. (C) White blood cell (WBC) count in GFP⁺ cells of PB of AMKL mice. (D) The sizes of spleens and livers on day 15. (E) Spleen weight of AMKL mice on day 15. (F) Live weight of AMKL mice on day 15. (G) Giemsa-stained blood smear of AMKL mice. $n = 4$ per group. Error bars represent mean \pm SD. p values by two-way ANOVA in A, B and C. p values by one-way ANOVA in E and F. * $p < 0.05$, ** $p < 0.01$, *** $p < 0.001$ and **** $p < 0.0001$, as compared to vehicle.

AUTHOR CONTRIBUTIONS

Fuping Wang, Haotian Zhang and Binghong He contributed equally. Qiong Yang and Haitao Wang are co-corresponding authors. Fuping Wang, Haotian Zhang, HW, Binghong He, Zihan Liu, Xinxin Wu, Yuankai Liu, Xin Xu, Xiaoxue Gou and Qiong Yang performed experiments or wrote the paper.

ACKNOWLEDGMENTS

Thanks to Qiang Jeremy Wen and John D Crispino. This research was supported by the Natural Science Foundation of China Beijing Municipality (No. 2202021) and the National Natural Science Foundation of China (No. 22072005, 21773015).

CONFLICT OF INTEREST

The authors declare no competing interests.

DATA AVAILABILITY STATEMENT

The data that support the findings of this study are available from the corresponding author upon reasonable request.

ETHICS STATEMENT

All procedures followed were in accordance with the ethical standards of the Ethical Committee on Animal Experimentation of Beijing Normal University.

ORCID

Qiong Yang  <https://orcid.org/0000-0002-0420-3564>

PEER REVIEW

The peer review history for this article is available at <https://publons.com/publon/10.1002/hon.3110>.

REFERENCES

- Tefferi A. Primary myelofibrosis: 2021 update on diagnosis, risk-stratification and management. *Am J Hematol.* 2021;96(1):145-162. <https://doi.org/10.1002/ajh.26050>
- Gangat N, Marinaccio C, Swords R, et al. Aurora kinase A inhibition provides clinical benefit, normalizes megakaryocytes, and reduces bone marrow fibrosis in patients with myelofibrosis: a phase I trial. *Clin Cancer Res.* 2019;25(16):4898-4906. <https://doi.org/10.1158/1078-0432.ccr-19-1005>
- Venugopal S, Mascarenhas J. Current clinical investigations in myelofibrosis. *Hematol/Oncol Clin North Am.* 2021;35(2):353-373. <https://doi.org/10.1016/j.hoc.2020.12.003>
- Wang X, Hoffman R. What are the molecular mechanisms driving the switch from MPNs to leukemia? *Best Pract Res Clin Haematol.* 2021;34(1):101254. <https://doi.org/10.1016/j.beha.2021.101254>
- Arber DA, Orazi A, Hasserjian R, et al. The 2016 revision to the World Health Organization classification of myeloid neoplasms and acute leukemia. *Blood.* 2016;127(20):2391-2405. <https://doi.org/10.1182/blood-2016-03-643544>
- Wen QJ, Yang Q, Goldenson B, et al. Targeting megakaryocytic-induced fibrosis in myeloproliferative neoplasms by AURKA inhibition. *Nat Med.* 2015;21(12):1473-1480. <https://doi.org/10.1038/nm.3995>
- Jurgielewicz BJ, Yao Y, Stice SL. Kinetics and specificity of HEK293T extracellular vesicle uptake using imaging flow cytometry. *Nanoscale Res Lett.* 2020;15(1):170. <https://doi.org/10.1186/s11671-020-03399-6>
- Morita S, Kojima T, Kitamura T. Plat-E: an efficient and stable system for transient packaging of retroviruses. *Gene Ther.* 2000;7(12):1063-1066. <https://doi.org/10.1038/sj.gt.3301206>
- Gu H, Shi X, Liu C, et al. USP8 maintains embryonic stem cell stemness via deubiquitination of EPG5. *Nat Commun.* 2019;10(1):1465. <https://doi.org/10.1038/s41467-019-09430-4>
- Li J, Zhu H.-J. Liquid chromatography-tandem mass spectrometry (LC-MS/MS)-based proteomics of drug-metabolizing enzymes and transporters. *Molecules.* 2020;25(11):2718. <https://doi.org/10.3390/molecules25112718>
- Han C, Gu H, Wang J, Lu W, Mei Y, Wu M. Regulation of L-threonine dehydrogenase in somatic cell reprogramming. *Stem Cells.* 2013;31(5):953-965. <https://doi.org/10.1002/stem.1335>
- Grisouard J, Shimizu T, Duek A, et al. Deletion of Stat3 in hematopoietic cells enhances thrombocytosis and shortens survival in a JAK2-V617F mouse model of MPN. *Blood.* 2015;125(13):2131-2140. <https://doi.org/10.1182/blood-2014-08-594572>
- Abu-Elsaad NM, Serrya MS, El-Karef AM, Ibrahim TM. The heat shock protein 90 inhibitor, 17-AAG, attenuates thioacetamide induced liver fibrosis in mice. *Pharmacol Rep.* 2016;68(2):275-282. <https://doi.org/10.1016/j.pharep.2015.08.015>
- Newman B, Liu Y, Lee HF, Sun D, Wang Y. HSP90 inhibitor 17-AAG selectively eradicates lymphoma stem cells. *Cancer Res.* 2012;72(17):4551-4561. <https://doi.org/10.1158/0008-5472.can-11-3600>
- Rao R, Lee P, Fiskus W, et al. Co-treatment with heat shock protein 90 inhibitor 17-dimethylaminoethylamino-17-demethoxygeldanamycin (DMAG) and vorinostat: a highly active combination against human mantle cell lymphoma (MCL) cells. *Cancer Biol Ther.* 2009;8(13):1273-1280. <https://doi.org/10.4161/cbt.8.13.8726>
- Hertlein E, Wagner AJ, Jones J, et al. 17-DMAG targets the nuclear factor-kappaB family of proteins to induce apoptosis in chronic lymphocytic leukemia: clinical implications of HSP90 inhibition. *Blood.* 2010;116(1):45-53. <https://doi.org/10.1182/blood-2010-01-263756>
- Wen Q, Goldenson B, Silver Serena J, et al. Identification of regulators of polyploidization presents therapeutic targets for treatment of AMKL. *Cell.* 2012;150(3):575-589. <https://doi.org/10.1016/j.cell.2012.06.032>
- Liu GW, Hu XL, Sun B, et al. Phosphatase Wip1 negatively regulates neutrophil development through p38 MAPK-STAT1. *Blood.* 2013;121(3):519-529. <https://doi.org/10.1182/blood-2012-05-432674>
- Zhang Q, Jin H, Chen L, et al. Effect of ultrasound combined with microbubble therapy on interstitial fluid pressure and VX2 tumor structure in rabbit. *Front Pharmacol.* 2019;10:716. <https://doi.org/10.3389/fphar.2019.00716>
- Roh JL, Kim EH, Park HB, Park JY. The Hsp90 inhibitor 17-(allylamino)-17-demethoxygeldanamycin increases cisplatin antitumor activity by inducing p53-mediated apoptosis in head and neck cancer. *Cell Death Dis.* 2013;4(12):e956. <https://doi.org/10.1038/cddis.2013.488>
- Jhaveri K, Miller K, Rosen L, et al. A phase I dose-escalation trial of trastuzumab and alvespimycin hydrochloride (KOS-1022; 17 DMAG) in the treatment of advanced solid tumors. *Clin Cancer Res.* 2012;18(18):5090-5098. <https://doi.org/10.1158/1078-0432.ccr-11-3200>
- Katayama K, Noguchi K, Sugimoto Y. Heat shock protein 90 inhibitors overcome the resistance to Fms-like tyrosine kinase 3

- inhibitors in acute myeloid leukemia. *Oncotarget*. 2018;9(76):34240-34258. <https://doi.org/10.18632/oncotarget.26045>
23. Kim HJ, Gong MK, Yoon CY, et al. Synergistic antitumor effects of combined treatment with HSP90 inhibitor and PI3K/mTOR dual inhibitor in cisplatin-resistant human bladder cancer cells. *Yonsei Med J*. 2020;61(7):587-596. <https://doi.org/10.3349/ymj.2020.61.7.587>
 24. Lee HJ, Shin S, Kang J, et al. HSP90 inhibitor, 17-DMAG, alone and in combination with lapatinib attenuates acquired lapatinib-resistance in ER-positive, HER2-overexpressing breast cancer cell line. *Cancers*. 2020;12(9):2630. <https://doi.org/10.3390/cancers12092630>
 25. Wang L, Zhang Q, You Q. Targeting the HSP90-CDC37-kinase chaperone cycle: a promising therapeutic strategy for cancer. *Med Res Rev*. 2022;42(1):156-182. <https://doi.org/10.1002/med.21807>

SUPPORTING INFORMATION

Additional supporting information can be found online in the Supporting Information section at the end of this article.

How to cite this article: Wang F, Zhang H, He B, et al. Heat shock protein 90 inhibitors induce cell differentiation via the ubiquitin-dependent aurora kinase A degradation in a MPLW515L mouse model of primary myelofibrosis. *Hematol Oncol*. 2022;1-13. <https://doi.org/10.1002/hon.3110>